Instantaneous microwave frequency measurement system based on a simplest integrated microwave photonic filter

JIAHONG ZHANG[a, b, *], HAIYING LU[a, b], YINGNA LI[a, b], ZHENGANG ZHAO[a, b]
[a]*Faculty of Information Engineering and Automation, Kunming University of Science and Technology, Kunming 650504, China*
[b]*Yunnan Key Laboratory of Computer Technology Applications, Kunming 650504, China*

A simplest integrated microwave photonic filter (IMPF) is proposed and designed as an optical discriminator for instantaneous microwave frequency measurement (IMFM). Amplitude comparison functions (ACFs) of the IMFM system based on a Mach-Zehnder modulator (MZM) and a phase modulator (PM) are theoretically deduced and analyzed. Simulation results demonstrate that by designing the IMPF with lengths of L_1=0.5 mm and L_2=1 mm, and simultaneously tuning optical carrier of the MZM at one valley, one peak of the spectral response, the IMFM system with measureable range from DC to 35 GHz and ACF slope of 29 dB can be obtained. In addition, when using a PM, the monotonic frequency range is 0 Hz to 35.3 GHz with the ACF slope is 84.1 dB. However, from 4 GH to 32.1 GHz the ACF slope is only 17.6 dB. Both theoretical and simulation results indicate that based on such simplest IMPF a new approach with advantages of compact structure and better reconfigurability can be established for the IMFM.

(Received August 26, 2019; accepted June 16, 2020)

Keywords: Integrated optics, Microwave photonic filter, Instantaneous frequency measurement (IFM), Electro-optic (EO) modulation

1. Introduction

Microwave photonics has been considered as an enabling technology for generation, distribution, control, detection and measurement of microwave signals in arrears of biomedical, communication, electronic warfare, and aerospace based on its superior performances of large instantaneous bandwidth, wide frequency coverage, low phase noise, and strong immunity to electromagnetic interference (EMI) [1].

A photonic-assisted instantaneous microwave frequency measurement (IMFM) system consists the light source, the electro-optic modulator (EOM), the optical discriminator, the photo-detector (PD) and the post signal processing module. The EOM including the phase, intensity, polarization or electro-absorption modulator is utilized to load the frequency unknown microwave signal onto the optical carrier, the optical discriminator such as an optical comb filter, a fiber Bragg grating (FBG), a dispersion fiber, an integrated waveguide resonator, or an waveguide grating is used to map the unknown frequency into the optical power, the PD is used to convert the optical signal to electrical, and the microwave frequency can then be obtained through the post signal processing module [2, 10]. Power fading function of the microwave signal transmitting in a dispersive fiber [2, 3], optical filters [4, 5], and polarization interferometers [6, 8], and nonlinear optics [9, 10] have been used as different photonic discriminators to obtain the amplitude comparison function (ACF). Frequency-to-time mapping approach has also been proposed for measurement of multiple-frequency [11]. To improve stability and practicability of these bulky measurement system, on-chip photonic assisted measurement systems are researched recently [12, 15]. However, additional optical band pass filter, two optical lasers, an Erbium doped optical fiber amplifier (EDFA), a dual parallel Mach-Zehnder modulator (DPMZM), and a coarse wavelength-division multiplexer (CWDM) are required, which increases the system cost and complication.

In this paper, an instantaneous microwave frequency measurement (IMFM) system based on a simplest integrated microwave photonic filter (IMPF) as discriminator is proposed, designed, and analyzed. As the proposed IMPF has characteristics of simple structure, miniaturized size, and fully reconfigurable, the measurement system has distinct advantages of compact size, more robust against external disturbance, and better reconfigurability.

2. Operation principles

The schematic diagram of the proposed IMFM approach is shown in Fig. 1. As shown in Fig. 1, two parallel optical waveguides with different lengths but same width are fabricated on the same crystal substrate. A high reflective film is fabricated on the front facet of the substrate while the back facet is polished, which results in only a small part of optical signal is reflected from the back facet while most of the rest are transmitted forward and reflected from the front facet, and then the interferometric effect occurs via the interference between the signal reflected from the front facet and the one reflected from the back facet. As a result, the interferometric effect occurs at the front facet can be treated as the so called two-beam interference or the Michelson like interference but not the Fabry-Perot

interference [16, 17]. However, only the front waveguide facet is fabricated with reflective film is due to the fact that if a high reflective film is fabricated on the back facet, the fiber-waveguide coupling cannot be achieved as the optical path is almost blocked by the reflective film. Besides, the reflective film coated on the back fact is used to offset the waveguide transmission loss to make it possible that magnitudes of the two reflected waves are as equal as possible such that a higher interference extinction ratio can be generated.

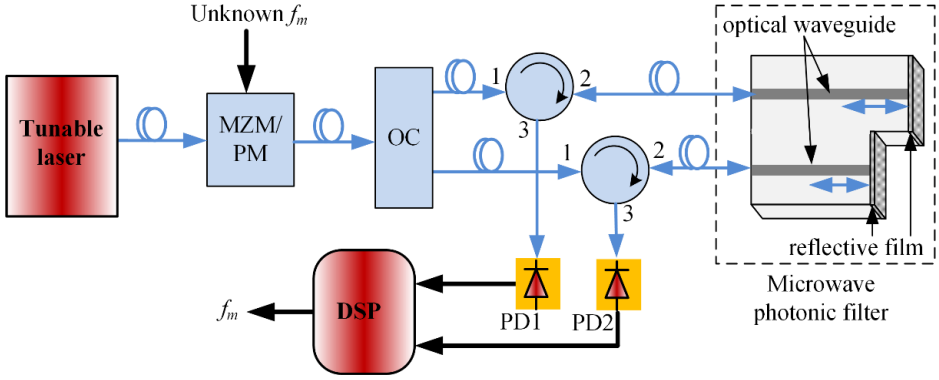

Fig. 1. Schematic diagram of the proposed IMFM approach. (f_m, frequency of the microwave signal; MZM, Mach-Zehnder modulator; PM, phase modulator; PD, photo-detector; OC, optical coupler) (color online)

The output optical power P_{out} of such IMPF can then be expressed as

$$P_{outk} = \frac{1}{4} P_o \alpha_k [1 + b_k \cos(\frac{4\pi}{\lambda} n_{eff} L_k)] \tag{1}$$

where, P_o is the output optical power of the tunable laser, α_k (k=1, 2) is the loss factor of the two optical paths from the optical couplers (OC) to the photo-detectors (PD), L_k (k=1, 2) are lengths of the two optical waveguides, and $b_k = \frac{P_{outk\max} - P_{outk\min}}{P_{outk\max} + P_{outk\min}} = \frac{2R_1R_2(1-\beta_k)(1-R_1)}{R_1^2 + (1-\beta_k)^2(1-R_1)^2R_2^2}$ (R_1, R_2 are the reflective coefficients of the front and back facts, and β_k are the loss factors of the two optical waveguides) are the extinction ratios of the IMPF. However, in Eq. (1), the phase shift on reflection which is decided by the reflectivity of the reflective film and the one-way phase factor is ignored due to the fact that the one-way phase factor is zero for the proposed IMPF [17].

From Eq. (1), based on such simplest structure, two microwave photonic filters with different sinusoidal responses are designed and fabricated on a single chip, which is the proposed IMPF. Based on such IMPF, two IMFM measurement systems using MZM and PM to load the frequency unknown microwave signal are proposed. The detailed principles are derived as follows:

(1) A MZM is used to load the frequency unknown microwave signal

By using a Mach-Zehnder modulator (MZM) biased at the minimum transmission point (the optical carrier is completely suppressed) to connect the frequency unknown microwave signal. Under small signal model and neglecting the high-order sidebands, the output optical field consists only the two first-order sidebands with equal amplitudes and a same phase. The output optical field $E(t)$ can be written by

$$\begin{aligned} E(t) &= E_c \cos(\omega_c t)\cos[\delta\cos(\omega_m t) + \frac{\pi}{2}] \\ &= 2E_c \cos(\omega_c t)\sum_{n=1}^{\infty}(-1)^n J_{2n-1}(\delta)\cos[(2n-1)\omega_m t] \\ &\approx -2E_c J_1(\delta)\cos(\omega_c t)\cos(\omega_m t) \end{aligned} \tag{2}$$

where E_c, ω_c are the amplitude and frequency of the optical carrier, $\delta=\pi(V_m/2V_\pi)$ is the modulation index, V_π is the half-wave voltage of the MZM, ω_m, V_m are frequency and amplitude of the microwave signal, and $J_n(.)$ denotes a Bessel function of the first kind of order n.

By wavelength tuning to set the optical carrier ω_c at peak or valley of the spectral response of the IMPF, and considering the offset $\omega_c \pm \omega_m$ is the microwave frequency, the power transmission function H_k of the IMPF can then be written as

$$H_k = \frac{1}{2}[1 \pm b_k \cos(\frac{\omega_m}{F_k})] \tag{3}$$

where, $F_k=C/(2n_{eff}L_k)$ (k=1, 2) is the free spectral range (FSR) of the IMPF, C is the light speed in the vacuum, and n_{eff} is the effective refractive index of the optical waveguide.

According to Eq. (2) and Eq. (3), the output optical power $P_{out1,\ 2}$ of the IMPF carried with the unknown microwave frequency can be described as

$$P_{out1,2}(t) = \frac{1}{2} P_0 [J_1(\delta)]^2 \alpha_k [1 \pm b_k \cos(\frac{\omega_m}{F_k})] \tag{4}$$

Based on Eq. (4), and considering the transmission factors α_1, α_2 and the extinction ratios b_1, b_2 are theoretically approximately equal with each other, the ACF of the IMPF output optical signals of are written as

$$\begin{cases} \mathrm{ACF}_1 = \dfrac{1+b_1\cos(\frac{\omega_m}{F_1})}{1+b_1\cos(\frac{\omega_m}{F_2})} \\ \mathrm{ACF}_2 = \dfrac{1-b_1\cos(\frac{\omega_m}{F_1})}{1-b_1\cos(\frac{\omega_m}{F_2})} \\ \mathrm{ACF}_3 = \dfrac{1-b_1\cos(\frac{\omega_m}{F_1})}{1+b_1\cos(\frac{\omega_m}{F_2})} \end{cases} \tag{5}$$

where, ACF_1, ACF_2, ACF_3 are power ratios of the IMPF on condition of tuning the optical carrier ω_c at both the peak, both the valley, and at on peak, one valley of the two spectral responses respectively.

(2) A PM is used to load the frequency known microwave signal

As shown in Fig. 1, secondly, by using a phase modulator (PM) to connect the frequency unknown microwave signal, under small-signal condition, and neglecting the high-order sidebands, the output optical field $E(t)$ consists of only the optical carrier and the two first-order side bands with equal amplitudes but an opposite phase. This can be written as

$$\begin{aligned} E(t) &= E_c e^{j[\omega_c t + m\cos(\omega_m t)]} \\ &= E_c e^{j\omega_c t}\sum_{n=-\infty}^{\infty} j^n J_n(m) e^{jn\omega_m t} \\ &\approx E_c[J_0(m)e^{j(\omega_c t)} + J_1(m)e^{j[(\omega_c+\omega_m)t+\frac{\pi}{2}]} - \\ &\quad - J_1(m)e^{j[(\omega_c-\omega_m)t-\frac{\pi}{2}]}] \end{aligned} \tag{6}$$

where, as in Eq. (2), E_c, ω_c are the amplitude and frequency of the optical carrier, V_m, ω_m are the amplitude and frequency of the microwave signal, $J_n(.)$ denotes a Bessel function of the first kind of order n, $m=\pi(V_m/V_\pi)$ is the phase-modulation index, and V_π is the half-wave voltage.

Essentially, by using the IMPF, the phase and amplitude relations of the PM first-order sidebands are broken such that the phase modulation to intensity modulation (PM-IM) conversion occurs. With each frequency component is multiplied by a different frequency weight of $H_k(\omega)$, the output spectrum of the PM can be expressed as

$$\begin{aligned} E(\omega) = 2\pi E_c[&J_0(m)\sqrt{H_k(\omega_c)} + J_1(m)\sqrt{H_k(\omega_c+\omega_m+\frac{\pi}{2})} - \\ &- J_1(m)\sqrt{H_k(\omega_c-\omega_m-\frac{\pi}{2})}] \end{aligned} \tag{7}$$

After detecting of the square-law photodetector (PD) and neglecting the $J_n(.)^2$ term, the output alternative (ac) current component can be described as

$$\begin{aligned} i_{ac,k} \propto 4\pi^2 P_0 J_0(m) J_1(m)[&\sqrt{H_k(\omega_c)}\sqrt{H_k(\omega_c+\omega_m+\frac{\pi}{2})} - \\ &- \sqrt{H_k(\omega_c)}\sqrt{H_k(\omega_c-\omega_m-\frac{\pi}{2})}] \end{aligned} \tag{8}$$

where, as in Eq. (1), $P_0=E_c^2$ is output optical power of the tunable laser.

According to Eq. (8), ACF of the PDs detected ac components is expressed as

$$\mathrm{ACF}_4 = \frac{\sqrt{H_1(\omega_c)}\sqrt{H_1(\omega_c+\omega_m+\frac{\pi}{2})} - \sqrt{H_1(\omega_c)}\sqrt{H_1(\omega_c-\omega_m-\frac{\pi}{2})}}{\sqrt{H_2(\omega_c)}\sqrt{H_2(\omega_c+\omega_m+\frac{\pi}{2})} - \sqrt{H_2(\omega_c)}\sqrt{H_2(\omega_c-\omega_m-\frac{\pi}{2})}} \tag{9}$$

From Eq. (5) and Eq. (9), both the optical power and microwave power (the Bessel function) are eliminated, and only the ACF and the unknown microwave frequency has a monotonic relationship. Accordingly, the microwave frequency can be discriminated by monitoring the output powers of the IMPF.

In addition, in Eq. (4) the output optical power has no relationship with frequency, which means only two PDs with very low frequency are required to measure the DC optical power for such frequency-to-optical power mapping approach. The minimum detectable optical power P_0 and microwave power $[J_1(\delta)]^2$ is decided by the responsivity and drive voltage of the practical utilized PD and modulator. Usually, responsivity of the PIN type PD is 0.8~0.9 mA/mW and power of the microwave signal is 28.6 dBm to match the drive voltage (6 V) of the modulator.

3. Results and discussions

Using parameters included in Table. 1, two $LiNbO_3$ IMPFs are designed. The 6 μm waveguide width is designed to maintain the single mode transmission of light beam in the waveguide. The optical waveguide can be fabricated using current established technologies of photolithograph and annealed proton exchange.

Table. 1 Parameters of the designed two optical waveguide filters

L_k (mm)		n_{eff}	b_k	width (μm)	F_k (GHz)
IMPF one	1	2.13	0.9	6	70.1
	0.5	2.13	0.9	6	140.2
IMPF two	6	2.13	0.9	6	11.7
	2	2.13	0.9	6	35.1

However, from Eq. (1), by designing the optical waveguide and reflective coefficients, the extinction ratio b_k can be changed. For example, if R_1=0.2, R_2=0.65, and β_k=0.4, b_k will be approximately equal to 0.91. In fact, consider the optical phase difference of the two light

beams reflected from the front and back facets is determined by size and length of the optical waveguide which is in fact depend on practical fabricated technology, b_k will affected by the waveguide fabrication technology as well. Based on the previous research on reflective optical waveguide Mach-Zehnder interferometer (MZI) [18], the IMPF with optical waveguide length from a few hundreds microns to a few centimeters and extinction ratio of more than 0.9 can be achieved under current optical waveguide fabrication technology.

According to Eq. (1), spectral responses of the designed two IMPFs are shown in Fig. 2. As can be seen from Fig. 2(a), when designing L_1=0.5 mm and L_2=1.0 mm (length ratio of the two optical waveguides is 1:2), it is possible to set the optical carrier at both the peak, or at one peak and one valley of the spectral responses by tuning wavelength of the tunable laser. For example, as shown in Fig. 2(a), when the output wavelength is tuned to 1549.25±(2p+1)·0.56 nm (p=0, 1, 2, 3…) and tuned to 1549.25±p·1.12 nm (p=0, 1, 2, 3…) the optical carrier is set at one valley, one peak and both peak of the spectral responses (point A and B) respectively. In addition, as shown in Fig. 2(b), when designing L_1=2 mm and L_2=6 mm (length ratio of the two optical waveguides is 1:3), and the output wavelength is tuned to 1549.1±(2p+1)·0.14 nm (p=0, 1, 2, 3…) and to 1549.25±p·0.28 nm (p=0, 1, 2, 3…), the optical carrier is set at both the peak and valley of the spectral responses (point B and C).

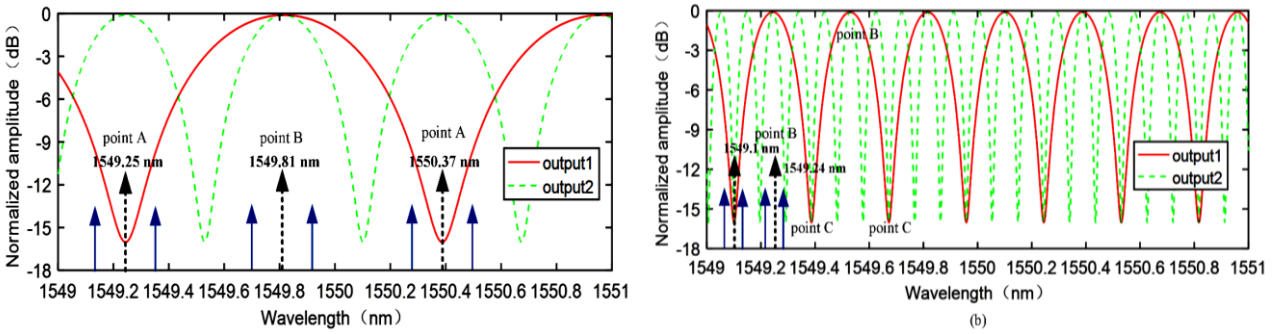

Fig. 2. Response of the two designed optical filters with (a) L_1=0.5 mm, L_2=1.0 mm, and (b) L_1=2 mm, L_2=6 mm (color online)

According to Eq. (5), ACF dependences on the input microwave frequencies are calculated and shown in Fig. 3. The ACF_1, ACF_2 and ACF_3 are responses on conditions of tuning the optical carrier at both the peak (point B), both the valley (point C), and to one peak and one valley (point A) of the two spectral responses respectively. From Fig. 3(a), for IMPF one with FSR of 70.1 GHz and 140.2 GHz, the microwave frequency monotonic range of ACF_1 and ACF_3 are 0-35.0 GHz and 0-35.0 GHz, while the corresponding slopes are 13.0 dB and 29.0 dB. In addition, as shown in Fig. 3(b), for IMPF two with FSR of 11.7 GHz and 35.1 GHz, the microwave frequency monotonic range of ACF_1 and ACF_2 are 0-5.8 GHz and 8.9-11.6 GHz, while the corresponding slopes are 14.5 dB and15.0 dB respectively.

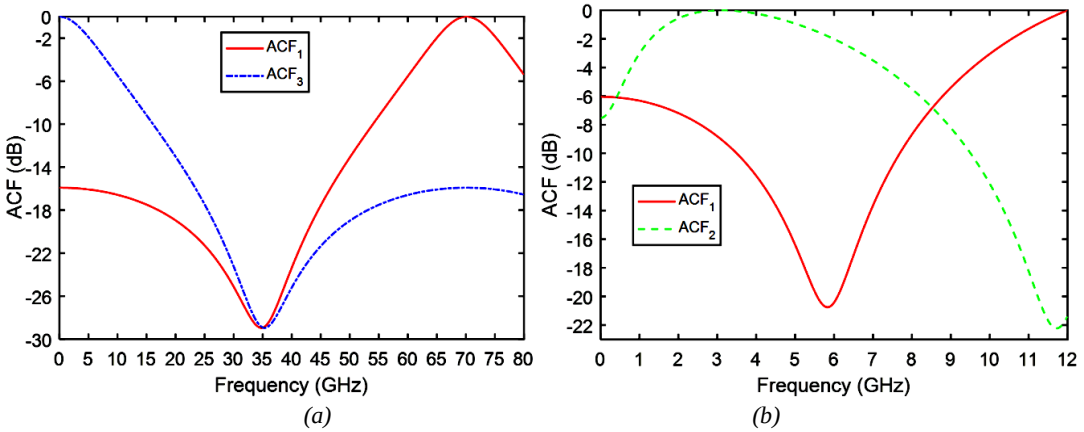

Fig. 3. Dependence of ACF on microwave frequency for the optical carrier tuned on the three points of the spectral response of (a) filter one and (b) filter two (color online)

Accordingly, the measureable frequency range is determined by the FSR of the IMPF, which means a wider measurement range can be achieved by designing shorter waveguide length. Moreover, the highest ACF slope can be obtained when the optical carrier is tuned to one peak and one valley of the spectral response of the IMPF. As a result, there is not any trade off or limitation between the measurement range and slope with size of the IMPF so

that the measurement system can become more compact and hence more robust against external disturbance.

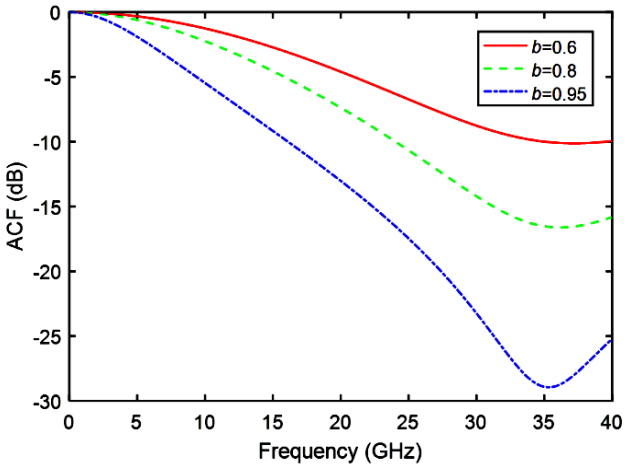

Fig. 4. Dependence of ACF on microwave frequency for different extinction ratios (color online)

Furthermore, Fig. 4 investigates dependences of ACF on the microwave frequencies for different extinction ratios, when the optical carrier is tuned on one peak, one valley of the spectral response of IMPF one. From Fig. 4, for the extinction ratios are 0.6, 0.8, and 0.95, the ACF increases monotonically from 0 to 35 GHz, while the ACF slopes are 10.0 dB, 16.7 dB and 29.0 dB respectively. The extinction ratio of the IMPF affects the ACF slope extensively but not the measurement range.

Consider the minimum waveguide length and maximum extinction ratio are mainly determined by the practical optical waveguide fabrication technology and material. Under current $LiNbO_3$ optical waveguide fabrication technology, the IMPF with minimum length of dozens of micron and extinction ratio greater than 0.9 can be acquired. Consequently, the IMFM system with measureable microwave frequency up to tens or hundreds of gigahertz and ACF slope up to tens of dB can be established. Besides, the measurement performances can be reconfigurable by using such IMPF with programmable optical waveguide length and extinction ratio.

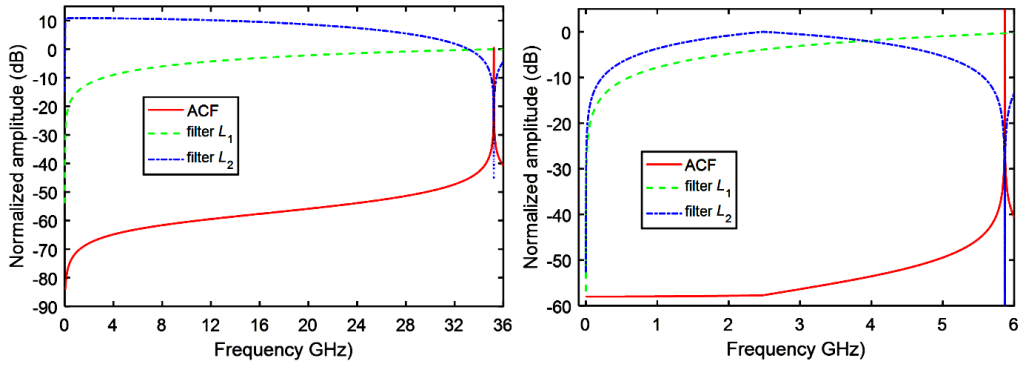

Fig. 5. Dependence of ACF on microwave frequency for a PM is used (a) with filter one and (b) with filter two (color online)

Secondly, a PM is used to receive the frequency unknown microwave signal. As shown in Fig. 2, by tuning the optical carrier deviates from the peak and valley of the spectral response, for example tuning the optical carrier to 1549.37 and 1549.11 nm respectively for IMPF one and two. Based on Eq. (9), dependence of ACF on microwave frequency is calculated and shown in Fig. 5. As shown in Fig. 5, the monotonic ACF ranges are 0-35.3 GHz and 0-5.9 GHz based on IMPF one and two, while the corresponding slope are 84.1 dB and 58.1 dB respectively. However, the ACF slopes are only 17. 6 dB and 8.6 dB respectively from 4.0 GHz to 32.1 GHz and 0 Hz to 5.0 GHz. Therefore, the IMFM system using a PM exhibits as well a programmable measurable range but a slower slope and lower measurement resolution.

Results of the two IMFM systems are compared in Table 2. As can be seen, the measurable frequency ranges of the two systems are determined by FSR of the IMPF which is subject to the waveguide length. By tuning optical carrier of the MZM at peak, valley, and one peak, one valley of the spectral response, the measurement slopes and ranges can be reconfigurable. For example, by tuning the optical carrier at one valley, one peak of the spectral response, the IMFM system with measureable range from DC to 35 GHz and ACF slope of 29 dB is obtained. However, for the IMFM system based on a PM, the ACF slope is higher than that of the system using a MZM in the overall frequency measureable range, but is lower in a wider part of frequency range. For example, the ACF slope is up to 84.1 dB in the overall frequency measurement range from 0 Hz to 35.3 GHz, but is only 17.6 dB from 4 GH to 32.1 GHz. As a result, resolution of such measurement system using a PM is lower than using a MZM.

Table 2. Calculation results of the IMFM approach based on MZM and PM

Electro-optic modulator	Microwave photonic filter	Optical carrier position	Frequency measurement range (GHz)	ACF response slop (dB)
Mach-Zehnder modulator (MZM)	L_1=0.5 mm, L_2=1 mm	peak	0-35.0	13.0
		one peak, one valley	0-35.0	29.0
	L_1=2 mm, L_2=6 mm	peak	0-5.8	14.5
		valley	8.9-11.6	15.0
Phase modulator (PM)	L_1=0.5 mm, L_2=1 mm	-	0-35.3 (total)	84.1 (total)
			4-32.1 (part)	17.6 (part)
	L_1=2 mm, L_2=6 mm	-	0-5.9 (total)	58.1 (total)
			0-5 (part)	8.6 (part)

Besides, for the proposed IMPF, more straight optical waveguides with different lengths can be designed and fabricated on a same $LiNbO_3$ substrate to form an IMPF array. As a result, by using an optical switch with multiple outputs to switch to different optical waveguides, the IMFM system with different performances can be setup.

4. Conclusions

In conclusion, a simplest IMPF formed by two straight optical waveguides with different lengths are proposed and designed. Utilizing two of such IMPFs with different FSR as frequency discriminators, two IMFM systems based on the MZM and PM are established. ACF of the IMFM system on different conditions are theoretically deduced and analyzed. Both theoretical and simulation results verify that the measurement range is mainly determined by FSR of the IMPF while the ACF slope is affected extensively by the EO modulation methods and conditions. By designing the IMPF with lengths of L_1=0.5 mm and L_2=1 mm, and simultaneously tuning the MZM optical carrier at one valley, one peak of the spectral responses, the IMFM measureable range system is calculated from DC to 35 GHz while the ACF slope is 29 dB. However, for the IMFM system using a PM, the ACF monotonic frequency range is 0 Hz to 35.3 GHz while the ACF slope is 84.1 dB in the overall measureable frequency but is only 17.6 dB from 4 GH to 32.1 GHz. All these results demonstrate that the proposed measurement system has potential capability to be used for instantaneous microwave frequency measurement, and the system compactness, robustness and reconfigurability are improved by using such simplest IMPF.

Acknowledgements

This study was supported by National Natural Science Foundation of China (Grant No. 61765009), the Applied Basic Research Project of Yunnan province (Grant No. 2018FB106), and the Introducing Talent Research Start-up Project of KMUST (Grant No.KKSY201603042).

References

[1] J. B. Tsui. Microwave Receivers with Electronic Warfare Applications, Wiley, New York, 1986.
[2] L. V. T. Nguyen, D. B. Hunter, IEEE Photonics Letters **18**, 1188 (2006).
[3] Y. Chen, B. Yang, H. Chi, X. Jin, S. Zheng, X. Zhang, Optics Communications **292**, 53 (2013).
[4] H. Chi, X. Zou, J. Yao, IEEE Photonics Technology Letters **20**, 1249 (2008).
[5] X. Zou, W. Pan, B. Luo, L. Yan, IEEE Photonics Technology Letters **23**, 39 (2011).
[6] Z. Tu, A. Wen, Y. Gao, W. Chen, Z. Peng, M. Chen, IEEE Photonics Technology Letters **28**, 2795 (2016).
[7] X. Li, A. Wen, X. Ma, W. Chen, Y. Gao, W. Zhang, Applied Optics **55**, 8727 (2016).
[8] B. Zhang, X. Wang, S. Pan, Journal of Lightwave Technology **36**, 2589 (2018).
[9] B. Lam, A. Mitchell, Optics Express **21**, 8550 (2013).
[10] H. Emami, M. Ashourian, IEEE Transactions on Microwave Theory & Techniques **62**, 2462 (2014).
[11] T. A. Nguyen, E. H. W. Chan, R. A. Minasian, Optics Letters **39**, 2419 (2014).
[12] D. Marpaung, IEEE Photonics Technology Letters **25**, 837 (2013).
[13] L. Liu, H. Qiu, Z. Chen, Z. Yu, IEEE Photonics Journal **9**, 1 (2017).
[14] M. Pagani, B. Morrison, Y. Zhang, A. Casas-Bedoya, T. Aalto, M. Harjanne, M. Kapulainen, B. J. Eggleton, D. Marpaung, Optica **2**, 751 (2015).
[15] H. Jiang, Optica **3**, 30 (2016).
[16] K. T. V. Grattan, B. T. Meggitt, Optical Fiber Sensor Technology (Fundamentals), Boston: K1uwer Academic Publisher, 2000.
[17] M. Yang, C. Gu, J. Hong, Optics Letters **24**, 1239 (1999).
[18] J. Zhang, C. Luo, G. Zhao, Journal of Lightwave Technology **37**, 1440 (2019).

* Corresponding author: zjh_mit@163.com